Cancer Management and Research

Elevate Series

Open Access Full Text Article

ORIGINAL RESEARCH

Synergistic Inhibition of Angiogenesis and Tumor Progression by CD73 Inhibitor and Menstrual Blood Stem Cell-Derived Exosomes via miR-422a Upregulation in HER2-Positive Breast Cancer

Narges Jafarbeik Iravani[1], Keivan Majidzadeh-A[1], Samaneh Arab[2,3], Shiva Zarinfam[1], Farkhonde Hasannejad[1]

[1]Genetics Department, Breast Cancer Research Center, Motamed Cancer Institute, ACECR, Tehran, Iran; [2]Department of Tissue Engineering and Applied Cell Sciences, School of Medicine, Semnan University of Medical Science, Semnan, Iran; [3]Department of Pathology, School of Medicine, Semnan University of Medical Sciences, Semnan, Iran

Correspondence: Farkhonde Hasannejad, Genetics Department, Breast Cancer Research Center, Motamed Cancer Institute, ACECR, P.O. BOX: 15179/64311, Tehran, Iran, Tel +989369937419, Email 93it.hasannejad@gmail.com

Objective: HER2-positive breast cancer (HER2+ BC) remains an aggressive subtype with limited treatment efficacy due to therapeutic resistance and systemic toxicities. CD73, an ectoenzyme producing extracellular adenosine, promotes tumor progression by enhancing angiogenesis, immune evasion, and metastasis. Exosomes derived from menstrual blood mesenchymal stem cells (Exo-Mens) exhibit anti-tumor and anti-angiogenic effects through bioactive cargo delivery. This study investigated the synergistic therapeutic potential of CD73 inhibition (using APCP) combined with Exo-Mens in HER2+ BC, with particular focus on their effects on angiogenesis-related pathways and on the regulation of miR-20a and miR-422a.

Materials and Methods: SKBR3 HER2+ BC cells were treated with Exo-Mens, APCP, and their combination. Exosomes were isolated and characterized by TEM, DLS, and Western blotting. Cytotoxicity assays determined IC_{50} values and synergy indices. Functional assays (colony formation, scratch migration assay), flow cytometry for apoptosis, and qRT-PCR analysis of pro-angiogenic (HIF-1α, KDR), pro-invasive (NF-κB, MMP9), and microRNAs (miR-20a, miR-422a) were performed.

Results: APCP showed higher cytotoxic potency (IC_{50} = 12.41 μg/mL) than Exo-Mens (IC_{50} = 61.84 μg/mL). Combination therapy demonstrated strong synergy (combination index < 1), significantly reducing colony formation (10.41% vs. 100% in controls), and cell migration (26.13% wound closure vs. 100% control). Both treatments downregulated angiogenesis factors (HIF-1α, KDR), while invasion markers (NF-κB, MMP9) showed treatment-specific responses. Notably, miR-422a was significantly upregulated across treatments, with the highest fold-change in the combination (3.05 ± 0.05), whereas miR-20a showed only modest changes. Combination therapy also enhanced apoptosis (viable cells reduced to 46.2% vs. 89.1% control).

Conclusion: The combination of APCP and Exo-Mens demonstrated synergistic anti-tumor effects in HER2+ BC cells by targeting pathways related to angiogenesis, proliferation, and apoptosis. In this context, the upregulation of miR-422a suggests a potential tumor-suppressive role, warranting further investigation.

Plain Language Summary: CD73 inhibition combined with menstrual blood stem cell-derived exosomes synergistically suppressed proliferation, migration, and angiogenesis in HER2-positive breast cancer cells.

The combinational treatment downregulated HIF-1α and KDR expression while enhancing apoptosis, indicating multi-pathway anti-tumor effects.

miR-422a was significantly upregulated by all treatments, especially the combined approach, suggesting its potential role as a tumor-suppressive regulator in HER2-positive breast cancer.

Keywords: HER2-positive breast cancer, CD73 inhibitor, MenSC-exosomes, angiogenesis, miR-422a, synergistic therapy

https://doi.org/10.2147/CMAR.S581878
Received: 15 November 2025
Accepted: 2 March 2026
Published: 14 April 2026

Introduction

About 20% of breast cancers (BC) show an overexpression of the human epidermal growth factor receptor 2 (HER2), and the presence of HER2 has been associated with a poor prognosis.[1] Initial findings indicated that women diagnosed with HER2+ early breast cancer had a higher risk of recurrence and encountered worse survival rates compared to those with HER2-negative cancer. Hence, this subgroup is particularly important in both clinical and translational research, as conventional treatment modalities may sometimes be ineffective in achieving long-term disease management.[2] Therefore, the use of combination drugs, as well as recombinant therapies targeting HER2 receptors, is being investigated to increase therapeutic efficacy.[3,4]

For many years, chemotherapy with anthracyclines and taxanes was the standard treatment for all patients with HER2+ breast cancer. In addition, conventional therapies such as monoclonal antibodies and tyrosine kinase inhibitors, despite their curative effects, have been limited by systemic toxicity and acquired resistance. However, over the past two decades, a better understanding of tumor biology and the subsequent introduction of targeted therapies have significantly changed the approach to the management of HER2+ breast cancer, leading to improved survival rates.[5,6]

Among the emerging targets, CD73, also known as Ecto-5'-nucleotidase (NT5E), is a glycosylphosphatidyl inositol (GPI)-linked cell surface enzyme that has gained attention in cancer biology due to its function in converting extracellular AMP to adenosine.[7] This enzymatic activity contributes to the accumulation of adenosine in the tumor microenvironment (TME), which promotes tumor growth, metastasis, angiogenesis, and immune escape. High expression of CD73/NT5E has been observed in various malignancies, including breast, lung, colorectal, ovarian, gastric, and pancreatic cancers, and it correlates with poor prognosis and shorter overall survival.[8,9]

CD73, along with CD39, drives angiogenesis through adenosine signaling via A2A and A2B receptors, upregulating pro-angiogenic factors such as vascular endothelial growth factor (VEGF).[10,11] This process supports tumor vascularization and dissemination[11]. CD73 expression is tightly regulated by hypoxia, a hallmark of the TME, where hypoxia-inducible factors (HIFs) enhance its transcription, sustaining adenosine accumulation and enabling immune evasion.[12,13] Accumulating preclinical and translational evidence indicates a functional interplay between HER2 signalling and the CD73-mediated adenosinergic axis, whereby elevated CD73 activity in HER2-positive tumours promotes adenosine-driven immunosuppression and angiogenesis, thereby facilitating immune evasion and reducing sensitivity to anti-HER2 therapies such as trastuzumab.[14] Furthermore, CD73 expression patterns differ across breast cancer subtypes and are frequently elevated in hormone receptor–negative and HER2-positive tumors, highlighting its relevance as a therapeutic target in this aggressive subgroup.[15]

In this regard, attention has also increased to cellular and biological therapies, including menstrual blood-derived stem cells (MenSCs) and their derived exosomes. MenSCs represent a non-invasive, rapidly expandable, and low-immunogenicity source of therapeutic extracellular vesicles, whose exosome fraction has shown potent anti-angiogenic and anti-tumor activity in preclinical cancer models.[16] MenSC-exosomes (Exo-Mens) have been demonstrated to suppress tumor-associated angiogenesis by attenuating ROS-dependent NF-κB activation, downregulating HIF-1α, and reducing VEGF and bFGF expression in both tumor and endothelial cells, thereby inhibiting endothelial viability, migration, and tube formation.[17] The anti-angiogenic effects of Exo-Mens are attributed to their unique bioactive cargo, including miRNAs and proteins targeting key angiogenic pathways.

Recent findings highlight the crucial role of microRNAs in cancer biology, although the regulatory mechanisms of specific microRNAs remain partially unknown. Here, this study aimed to investigate the regulatory effects of microRNAs, specifically miR-20a and miR-422a, based on published bioinformatics databases and recent evidence.[18] These microRNAs play pivotal roles in modulating CD73 (NT5E) expression and cancer-related mechanisms. Based on the study by T. Kordaß et al, microRNAs 20a and 422a regulate NT5E expression through complex mechanisms, both directly and indirectly. They stated that miR-422a decreases NT5E expression both directly through binding to the 3′-UTR of NT5E mRNA and indirectly by targeting SMAD4.

On the other hand, miR-20a downregulates NT5E expression indirectly by inhibiting the transcription factors HIF1A and SMAD4.[18] Furthermore, the function of miR-20a, part of the miR-17-92 oncogenic cluster, in facilitating proliferation, angiogenesis, and immune evasion across different cancers, as well as the contribution of miR-422a in promoting

tumor cell survival and altering the TME, has been demonstrated.[19,20] Increasing evidence also suggests that miR-422a functions as a context-dependent tumor regulatory microRNA through its modulation of key oncogenic and hypoxia-related pathways; however, its role in HER2-positive breast cancer remains largely unexplored.[21] Because the functional role of these microRNAs appears to be context-dependent and has not yet been fully elucidated, it is necessary to investigate their role in BC HER2+ cancer to clarify their biological significance.

Despite increasing evidence on CD73 signaling and exosome-based therapies, few studies have examined their combined effects in HER2-positive breast cancer, particularly with respect to microRNA-mediated regulation of angiogenic pathways. These gaps highlight the need for integrative therapeutic strategies targeting both metabolic and post-transcriptional regulatory mechanisms. Hence, the present study aimed to investigate the synergistic role of the CD73 inhibitor (APCP) and Exo-Mens in HER2-positive BC, and to evaluate miR-20a/miR-422a expression to provide new perspectives for targeted and personalized cancer therapy.

Materials and Methods

Materials

In our study, Adenosine 5'-(α, β-methylene) diphosphate (APCP) was procured from Sigma Company (United Kingdom). The APCP was subsequently dissolved in phosphate-buffered saline (PBS) with 20% dimethyl sulfoxide (DMSO). AnaCell commercial kit (Tehran, Iran) and the Bradford assay (Yektatajhiz, Tehran, Iran) were used for exosome isolation and concentration assessment, respectively. To assess cell viability, dimethyl sulfoxide (DMSO) and 3-(4, 5-dimethylthiazol-2-yl)-2, 5-diphenyl-2H-tetrasolium bromide (MTT) (Merck, Germany) were used.

Cell Culture

SKBR3 (human HER2+ Breast cancer) was purchased from Motamed Cancer Institute (Tehran, Iran). All cell lines were cultured in Dulbecco's modified Eagle's medium/F-12 (DMEM/F-12; Gibco, USA) containing 10% fetal bovine serum (FBS), 10 U/mL penicillin, and 10 μg/mL streptomycin in a humidified atmosphere with 5% CO_2 at 37°C.

Bioinformatic Analysis

A bioinformatics analysis was conducted to identify and characterize mRNAs and microRNAs that are associated with angiogenesis. Initially, gene sets associated with angiogenesis were obtained from recognized pathway databases, such as KEGG (Kyoto Encyclopedia of Genes and Genomes) and WikiPathways, which offer curated and detailed pathway maps for cellular and molecular processes. These databases facilitated the discovery of essential genes involved in angiogenesis by providing functional annotations and insights into their roles across various pathways.

Subsequently, various databases for microRNA target prediction and validation were utilized to investigate the possible regulatory microRNAs that target these genes associated with angiogenesis. TargetScan was employed for the in silico prediction of microRNA binding sites located on the 3' untranslated regions (3' UTRs) of the specified genes. Furthermore, validated interactions were corroborated through databases such as miRTarBase, which aggregates experimentally validated microRNA-target interactions; MirDB, for computational predictions; and the Human Protein Atlas, for context on tissue-specific gene and protein expression relevant to angiogenesis. To explore the possible functional interactions and network structure among the identified genes related to angiogenesis, a protein–protein interaction (PPI) analysis was conducted utilizing the STRING database (Search Tool for the Retrieval of Interacting Genes/Proteins). The integration of data from these varied sources provides a thorough understanding of the regulatory networks that influence angiogenic gene expression through microRNAs.

The Extraction and Analysis of Exo-Mens

To isolate exosomes derived from menstrual blood-derived mesenchymal stem cells (MenSCs), they were first purchased from the Royan Institute. The cells were characterized and confirmed for their specific positive (CD90+ and CD105+) and negative (CD45- and CD34-) CD markers to ensure their identity and purity. Briefly, MenSCs were cultured under standard conditions until reaching appropriate confluency, after which exosome secretion was induced by a 48-hour starvation period in a serum-

free medium (FBS-free conditions). The culture supernatant was collected, clarified by sequential centrifugation, and exosomes were isolated using a polyethylene glycol (PEG)-based precipitation method according to the manufacturer's instructions, as previously described in established protocols.[22,23] The isolated vesicles were resuspended in PBS and characterized using transmission electron microscopy (TEM), dynamic light scattering (DLS), and Western blotting for exosomal markers (CD9, CD81), consistent with the criteria recommended for exosome identification.[24]

Determination of the IC50 Value

To determine the optimal doses of Exo-Mens and the CD73 inhibitor (APCP), the SKBR3 cell line was cultured and subjected to the MTT (3-(4,5-dimethylthiazol-2-yl)-2,5-diphenyltetrazolium bromide) assay. Cells were cultured overnight in 96-well plates at a density of 5×10^3 cells per well. After 24 hours, the cells were treated with varying concentrations of Exo-Mens (400, 200, 100, 50, 25, 12.5, 6.25 μg/mL) and the APCP (200, 100, 50, 25, 12.5, 6.25, 3.125 μg/mL), followed by incubation for 48 hours under standard culture conditions. In addition, three wells were designated as controls and received no interventions. Subsequently, the MTT assay procedures were performed according to a previous study.[25] The absorbance of each well was measured at 570 nm using an optical absorption device (Biotek, USA) with a reference wavelength of 630 nm to account for background interference. The cell viability percentage was calculated using the following formula:

$$\text{Cell Viability}(\%) = \left(\frac{\text{Absorbance of treated cells} - \text{Absorbance of blank}}{\text{Absorbance of untreated cells} - \text{Absorbance of blank}}\right) \times 100$$

Finally, the IC50 was determined in SKBR3 cells using GraphPad Prism.

Calculating the Combined Dosage

Following the determination of IC50 values for Exo-Mens and APCP, their combined doses were evaluated by testing ratios of the compounds with coefficients ranging from 1 to 2 (Figure 1). These ratios were evaluated in 5 serial dilutions using the MTT assay to measure cell viability for SKBR3 cells. Data were analyzed with CompuSyn® software (ComboSyn Inc., Paramus, NJ, USA), which applies the Chou–Talalay method to quantify drug interactions.[26] This approach provides the combination index (CI) to classify interactions as synergistic (CI < 1), additive (CI = 1), or

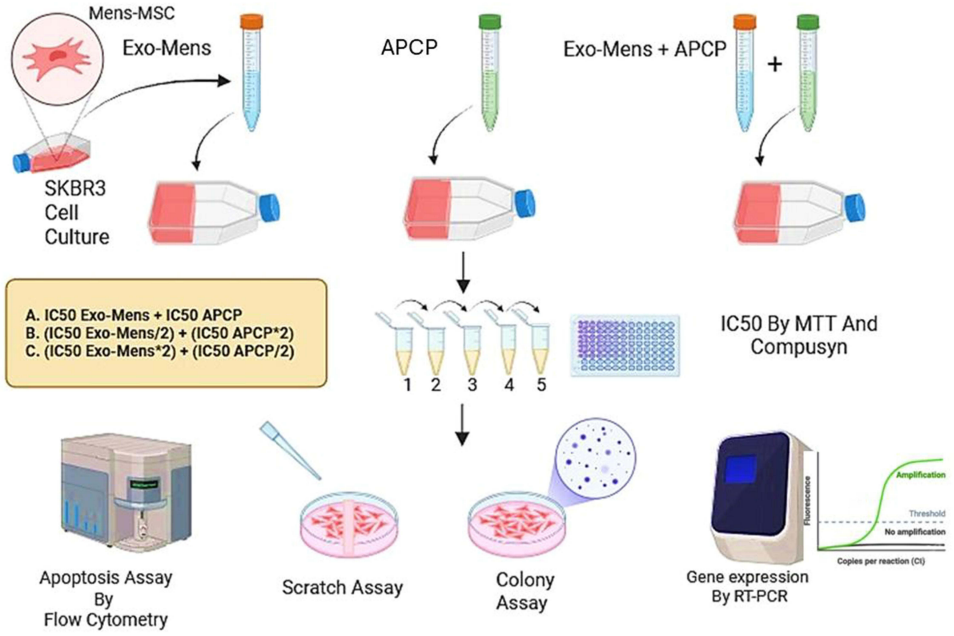

Figure 1 Overview of the methodological framework, showing the experimental protocol and the MTT-based evaluation of IC_{50} values for Exo-Mens, APCP, and their combined treatment.

antagonistic (CI > 1), and the dose-reduction index (DRI) to estimate potential dose reductions in combination treatments. Optimal combination ratios were selected based on maximal synergism and favorable DRI values for subsequent experiments.

In vitro Experiments

In this study, the SKBR3 cell line, a widely used model for HER2-positive breast cancer, was subjected to three distinct therapeutic interventions to evaluate their individual and combined effects. The experimental design included four groups: (1) Exo-Mens treatment, (2) APCP treatment, (3) combination therapy (Exo-Mens + APCP), and (4) a control group with no therapeutic intervention. Subsequently, the effective compounds were poured onto the cultured cells, and 48 hours later, the required cell assays were performed.

Colony Formation Assay

The cells' clonogenic ability (and their survival after treatment) were evaluated using a colony formation assay. In brief, 2×10^3 cells were plated in a 6-well plate. During the logarithmic growth phase, the culture medium was aspirated, and the cells were treated according to the specific experiments. After the treatment, cells were further incubated for 72 h for colony formation. Assessments were performed at 0, 24, 48, and 72 hours after treatment. The colonies were fixed in a 1.25% crystal violet solution afterwards. After gently washing off excess dye, colony images were obtained using a light microscope (Nova Tech Company, USA). The colony formation efficiency was calculated using Equation 1, as follows:

$$\text{Colonies}(\%) = \frac{\text{Number of colonies formed in treatment group}}{\text{Number of colonies formed in Control group}} \times 100$$

Scratch Assay

The migration of SKBR3 cells was assessed by wound healing (scratch) assay according to established protocols.[27] Cells were plated in 6-well plates and grown to 80% confluency under standard conditions. Specifically, to simulate a wound, a uniform linear scratch was created across the cell monolayer using a sterile 200 µL pipette tip. After the scratch, non-adherent cells were washed away with a gentle rinse in PBS, and cells were treated according to the desired treatment groups. Images were recorded using a phase-contrast microscope at specified time intervals to follow wound healing. To quantify cell migration, the number of migrated cells was counted in six fields per well. Image analysis was performed using ImageJ software (National Institutes of Health, Bethesda, MD, USA), allowing precise measurement of wound area and migration rate over time. Wound closure distance was measured and analyzed in accordance with Equation 2.

$$\text{Wound Closure}(\%) = \frac{[\text{A}(0\text{h}) - \text{A}(24\text{h})]}{\text{A}(0\text{h})} \times 100$$

Where A(0h) and A(24h) represent the initial and residual wound areas at 0 and 24 hours post-scratch, respectively.

RNA Extraction, Complementary DNA (cDNA) Synthesis, and Real-Time Polymerase Chain Reaction (RT-PCR)

Total RNA was extracted using RNX-PLUS reagent (Cinaclone, Iran) following the manufacturer's protocol. The concentration and purity of the isolated RNA were determined using a NanoDrop ND-2000 spectrophotometer (Thermo Fisher Scientific, Waltham, MA, USA). To evaluate RNA integrity, samples were subjected to agarose gel electrophoresis. For cDNA synthesis, polyadenylated RNA was first synthesized using Ratin Gene (Iran) reagents, according to the manufacturer's instructions. Subsequently, first-strand cDNA was synthesized using a cDNA synthesis kit (SMOBIO Technology, Taiwan), with 1000 ng of total RNA and poly(A)+ RNA as the input. Quantitative real-time PCR (qRT-PCR) was performed using the SYBR Green detection method with a final reaction volume of 10 µL. Each reaction contained 0.25 µL of 10 µM forward and reverse primers, 1 µL of cDNA, 5 µL of 2× SMOBIO qPCR master mix, and 3.5 µL of nuclease-free water. The thermal cycling conditions were as follows: an initial denaturation at 95°C for 30 seconds, followed by 40 amplification cycles of 95°C for 5 seconds and annealing at 60°C for 30 seconds for all

target genes. Reactions were performed in triplicate, and the relative gene expression levels were calculated using the ΔCt method. GAPDH and U48 served as endogenous reference genes. All primers were designed using GeneRunner software, validated using NCBI Primer-BLAST (https://www.ncbi.nlm.nih.gov/tools/primer-blast/), and synthesized by Pishgam Biotech (Iran) (Table S1). The specificity of amplification was confirmed by a single peak in the melting curve analysis, indicating the absence of nonspecific products or primer-dimer formation (Figure S1).

RNA purity and concentration were measured using a NanoDrop™ spectrophotometer at 260/280 nm. For microRNA analysis, cDNA synthesis was performed using the miScript II RT Kit (Qiagen), optimized for mature microRNAs. A cDNA synthesis kit (Yektatajhiz, Tehran, Iran) and SYBR Green (SMOBIO Technology, Inc.) were used to detect gene expression on a StepOnePlus™ Real-Time PCR System.

Apoptosis

Apoptotic cell death was evaluated using annexin V-FITC and propidium iodide (PI) dual staining followed by flow cytometry. SKBR3 cells (1×10^6) were treated with the experimental conditions for 48 hours. Both adherent and floating cells were collected, washed twice with cold PBS, and resuspended in 500 µL of annexin binding buffer. Cells were stained with 5 µL of annexin V-FITC and 5 µL of propidium iodide, incubated for 5 minutes at room temperature in the dark, and immediately analyzed using a flow cytometer (Roche Diagnostics, Basel, Switzerland) to quantify apoptotic and necrotic cell populations. A schematic overview of the study design and related assessments is presented in Figure 1.

Statistical Analysis

Statistical analysis was conducted using Minitab V17 and GraphPad Prism V7. All experiments were performed in at least three independent biological replicates unless otherwise specified. Comparisons between multiple experimental groups were performed using one-way analysis of variance (ANOVA) followed by Tukey's post hoc test for pairwise comparisons, which controls for multiple testing across groups. Data are presented as mean ± SD. Due to the exploratory nature of this in vitro study, no formal power analysis was performed; however, experiments were repeated independently to ensure reproducibility and minimize experimental variability. A p-value of < 0.05 was considered statistically significant (*).

Results

Network-Based Bioinformatics Analysis

The Wiki Pathways, KEGG databases, and several associated articles were utilized to identify genes implicated in the angiogenesis of breast cancer. Based on our results, green edges specifically represent direct associations between NT5E and other angiogenesis-related genes, including KDR, TEK, FGF2, PDGFRA, HIF1A, MYC, and notably ENTPD1. The ENTPD1 encodes CD39, an ectonucleoside triphosphate diphosphohydrolase that hydrolyzes extracellular ATP and ADP to AMP. Together, CD39 and CD73 constitute the major enzymatic pathway for extracellular adenosine production. In addition, two pivotal microRNAs, miR-20a-5p and miR-422a, were identified as post-transcriptional suppressors of central hub genes, including MYC, AKT1, and HIF1A, which are deeply involved in angiogenic signaling and tumor progression pathways. Finally, the relationships between the miRNAs and the identified potential target genes, as derived from the STRING database, are depicted in Figure 2.

Exo-Mens Characterization

Flow cytometric analysis for MenSCs-specific markers (CD90 and CD105 positive and CD34 and CD45 negative) was performed in a previous study,[28] and we used these characterized cells for exosome isolation. Evaluations related to the characterization of exosomes indicated an average particle size of 69.06 nm, which is within the recognized exosomal size range of 30 to 150 nm (Figure 3A). Furthermore, Western blot analysis confirmed the presence of exosome-specific markers CD9 and CD81, along with β-actin as a reference control (Figure 3B). As shown in Figure 3C, based on TEM analysis of Exo-Mens, it exhibited a spherical morphology and nanoscale size, consistent with the typical features of lipid bilayer vesicles.

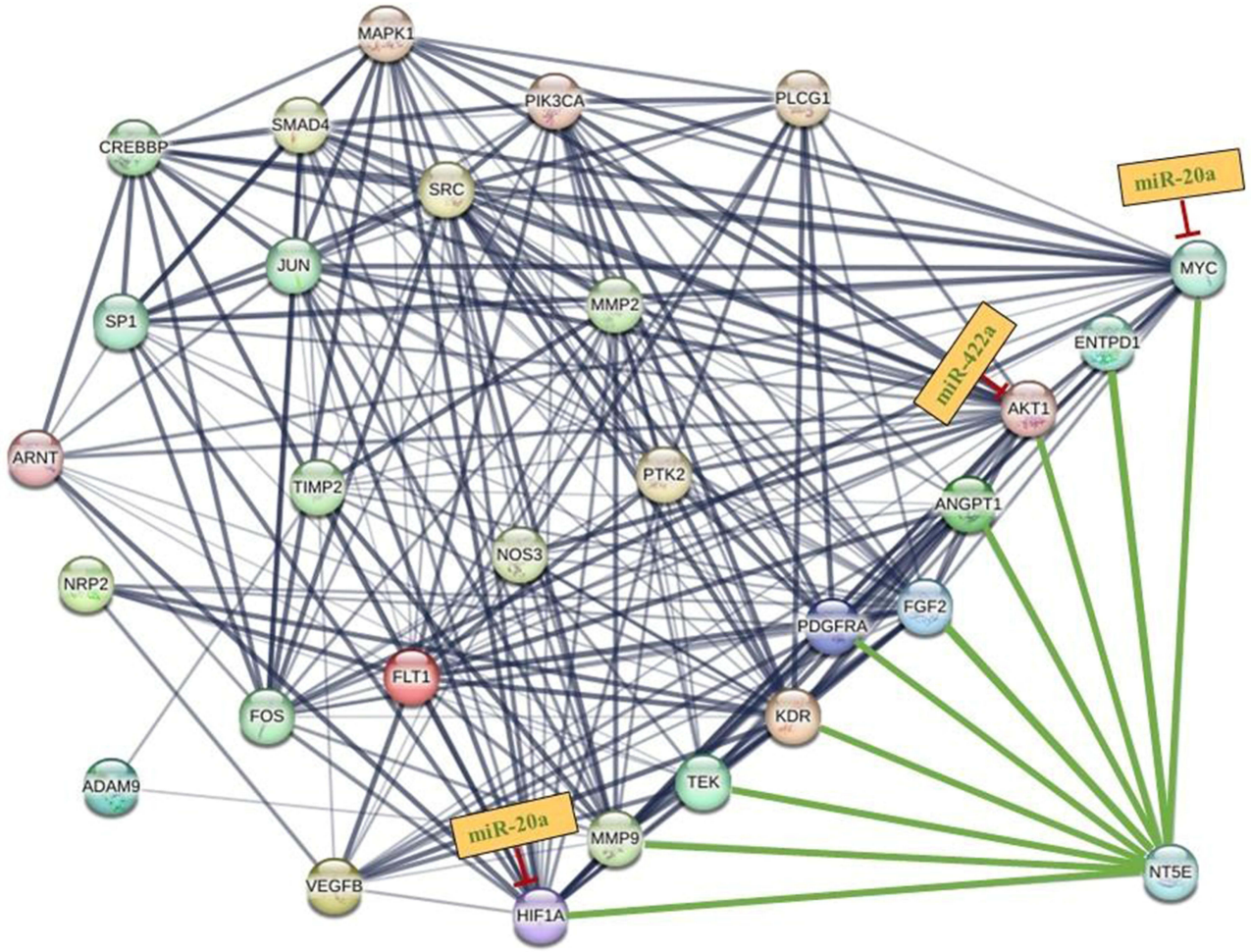

Figure 2 The network diagram illustrates gene interactions between NT5E (CD73) and key angiogenesis-related genes, generated using the STRING database. Dark (black) edges represent interactions curated from KEGG and WikiPathways databases. Edge thickness and color intensity correspond to the interaction confidence or strength among angiogenesis-related regulators, with darker and thicker edges indicating stronger predicted associations. In contrast, green edges specifically represent direct associations of NT5E with angiogenic regulators, including KDR, TEK, FGF2, AKT1, MYC, HIF1A, MMP9, PDGFRA, ANGPT1, and ENTPD1. Yellow boxes indicate the microRNAs miR-20a and miR-422a, which post-transcriptionally suppress central hub genes (MYC, HIF1A, AKT1) involved in angiogenic signaling. Network visualization was generated using STRING, with interaction data integrated from TargetScan, miRTarBase, and MirDB.

Determination of the IC50 Value and Combination Dose

The IC_{50} values of APCP and Exo-Mens in SKBR3 breast cancer cells were determined using the MTT assay, as illustrated in Figure 4. The results indicated that APCP exhibited a markedly lower IC_{50} than Exo-Mens, suggesting greater cytotoxicity and higher efficacy in reducing cell viability under the tested conditions.

To investigate the interaction between APCP and Exo-Mens, CompuSyn software was employed to analyze whether their combined effects were synergistic, additive, or antagonistic, as illustrated in Figure 5A. A range of concentrations for both APCP and Exo-Mens was evaluated, and the results demonstrated that their combined cytotoxic activity was significantly greater than when either compound was applied independently. Among all tested ratios, the combination of APCP/2 + Exo×2 emerged as the most potent, indicating superior efficacy compared to other mixing proportions. As shown in Table 1, the fraction affected (Fa) parameter denotes the proportion of inhibited cells, and the corresponding Combination Index (CI) values are calculated using the Chou-Talalay algorithm in CompuSyn software.[29] Synergy was primarily evaluated at Fa = 0.5 (corresponding to the IC_{50} and 50% viability inhibition), as indicated by the red rectangle.

By definition, CI = 1, <1, and >1 correspond to additive, synergistic, and antagonistic effects, respectively. According to the results, APCP/2 + Exo×2 displayed strong to moderate synergy for all Fa values, except for Fa = 0.05, 0.1, and 0.15, where synergy was not as pronounced. Additionally, as shown in Figure 5B, data points located below, above, or

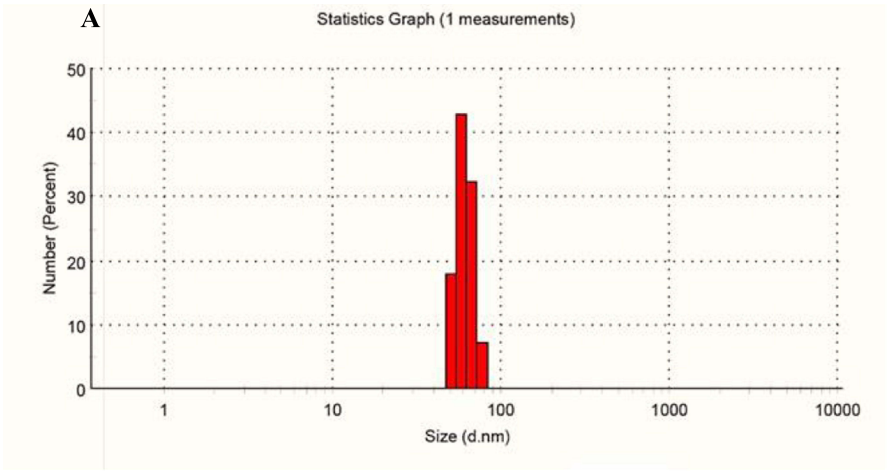

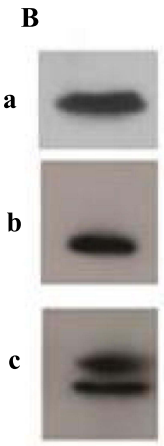

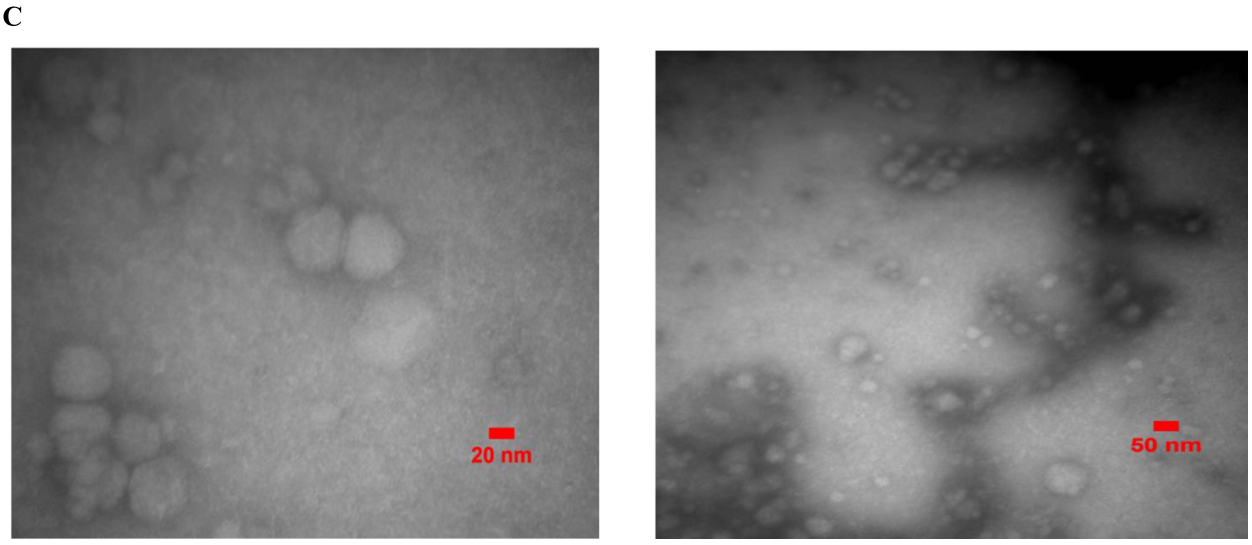

Figure 3 Characterization of Exo-Mens, including size distribution by DLS (**A**), Western blot verification of exosomal protein markers (**B**); bands correspond to: (**a**) β-Actin (42 kDa) serving as the loading control, (**b**) CD81 (34 kDa), (**c**) CD63 (26 kDa) and morphological analysis by TEM (**C**).

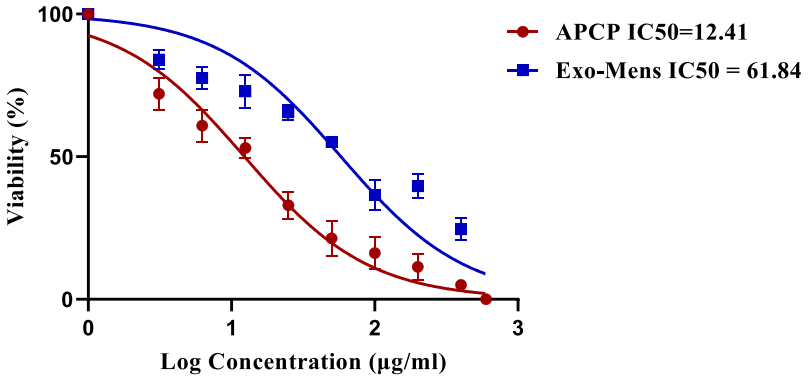

Figure 4 IC_{50} values of Exo-Mens and APCP in SKBR3 breast cancer cells. Results are presented as the mean of three independent replicates.

https://doi.org/10.2147/CMAR.S581878

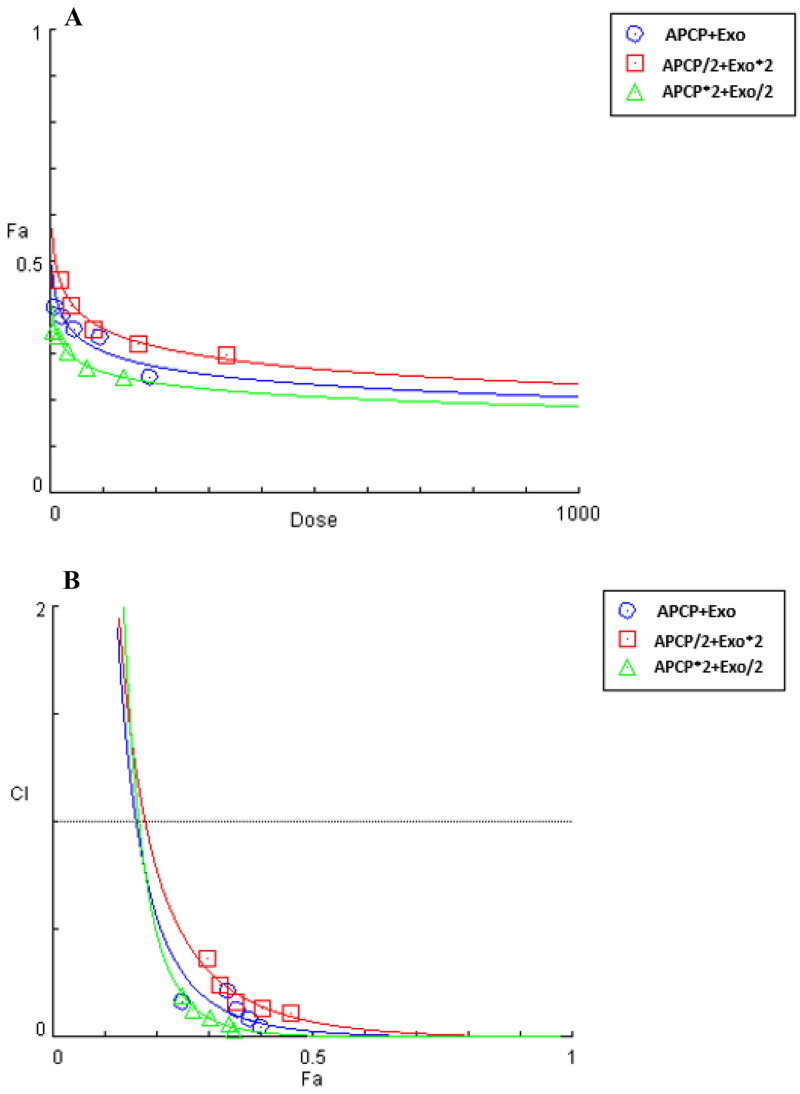

Figure 5 Dose–effect curves for Exo-Mens and APCP combinations at various ratios (**A**), and the Fa–CI plot derived from CompuSyn analysis for the corresponding combinations (**B**).

directly on the CI curve indicate synergistic, antagonistic, and additive interactions, respectively. For the optimal ratio of APCP/2 + Exo×2, which corresponds to 1:19.9, achieving Fa = 0.5 requires 0.4771 + 9.056 = 9.5332 units from APCP and Exo-Mens, respectively.

Colony Formation Assay

The colony formation assay showed that the control group formed more colonies than the treatment groups. Notably, the mean ± SD of colony formation for Exo-Mens, APCP, and APCP+Exo were 36.45 ± 1.30%, 16.47 ± 0.54%, and 10.41 ± 0.83%, respectively. These values showed a statistically significant difference compared to the control group (100%) (Figure 6). Consequently, SKBR3 cancer cells in the experimental groups exhibited reduced colony formation compared with the control group.

Scratch Assay

The scratch assay results demonstrated significant differences in wound closure efficiency among the four experimental groups: Control, Exo-Mens, APCP, and APCP+Exo. As expected, the Control group exhibited the highest percentage of wound closure at 72 h (100%), serving as the reference point for comparative evaluation. In contrast, treatment with Exo-

Table 1 CI Data for Combination APCP/2 + Exo×2 [1:19.9]

Fa	CI Value	Total Dose
0.05	11.1490	1,084,163
0.1	3.10008	56,502.1
0.15	1.40357	9071.95
0.2	0.77293	2288.91
0.25	0.47222	733.929
0.3	0.30705	271.723
0.35	0.20769	110.201
0.4	0.14407	47.3655
0.45	0.10144	21.0772
0.5	0.07194	9.53332
0.55	0.05102	4.31197
0.6	0.03592	1.91879
0.65	0.02492	0.82471
0.7	0.01686	0.33447
0.75	0.01096	0.12383
0.8	0.00670	0.03971
0.85	0.00369	0.01002
0.9	0.00167	0.00161
0.95	4.65E-4	8.38E-5
0.97	1.87E-4	1.02E-5

Notes: The red box denotes the Combination Index (CI) value at Fa = 0.5 (corresponding to the fraction affected at the median effective dose/IC_{50}, i.e., 50% inhibition of cell viability) in CompuSyn analysis.

Mens led to a marked reduction in cell migration, as indicated by the slower closure of the scratch area (31.7±2.3%, P). Treatment with APCP also further suppressed cell motility, resulting in less wound closure compared to the control group (32.5± 3.1%). Importantly, the combination of APCP and Exo-Mens resulted in the most effective wound closure, leaving the scratch area largely unfilled (26.13± 2.2%) (for all treatment P<0.001) (Figure 7).

Rt-Pcr

A comparative analysis of gene expression demonstrated distinct regulatory patterns among the angiogenesis-related genes (HIF-1α and KDR) and the invasion-associated genes (MMP9 and NF-κB) across the experimental groups. Both HIF-1α and KDR showed a statistically significant reduction in all treatment groups compared with the control ($P < 0.001$ for all), indicating a consistent anti-angiogenic effect of the interventions (Figure 8A and B). In contrast, the expression profiles of MMP9 and NF-κB exhibited treatment-dependent variability (Figure 8C and D). Specifically, in the Exo-Mens-treated group, although NF-κB expression decreased slightly compared to the control, the difference was not statistically significant ($P = 0.06$). Additionally, analysis of MMP9 gene expression in the Exo-Mens-treated group revealed increased expression compared to the control group ($P < 0.001$). Conversely, in the APCP-treated group, there was a notable decrease in the expression levels of NF-κB ($P=0.01$) and MMP9 ($P < 0.001$) genes in comparison to the control, implying a potential inhibitory effect on tumor invasion and progression. Interestingly, in the combination group (APCP+Exo), MMP9 expression increased ($P<0.001$), suggesting a complex regulatory or compensatory response to the combination treatment protocol. However, the expression level of NF-κB did not show a statistically significant difference compared to the control group ($P = 0.07$) (Figure 8C and D).

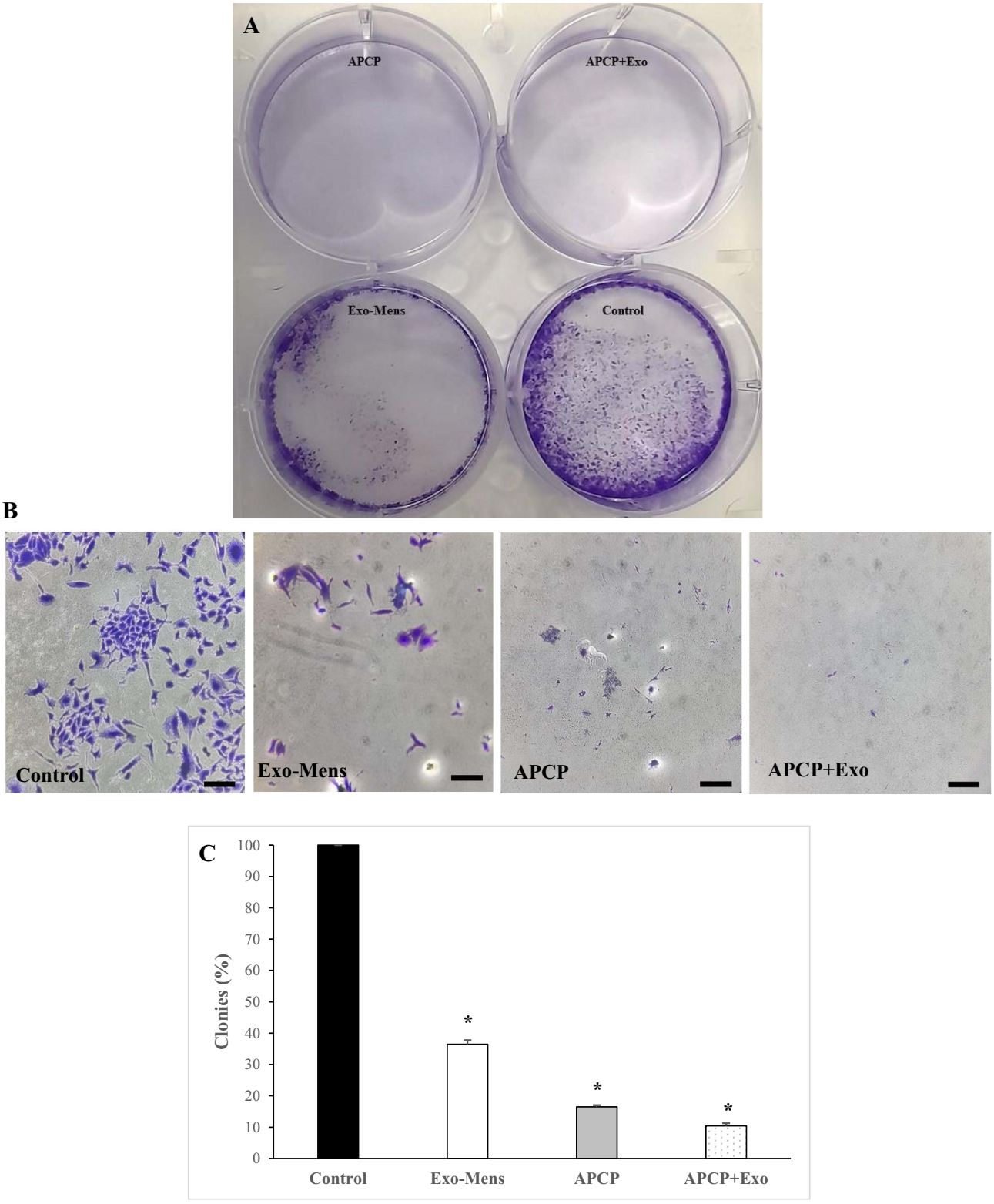

Figure 6 Clonogenic assay demonstrating the effects of control, Exo-Mens, APCP and APCP+ Exo treatments on colony formation: representative colony plates (**A**), microscopic images (**B**), and quantitative analysis of SKBR3 cells (**C**). Data are expressed as mean ± SEM from three replicates across five randomly selected fields. Scale bars = 200 μm. *p < 0.001 vs. control group.

https://doi.org/10.2147/CMAR.S581878

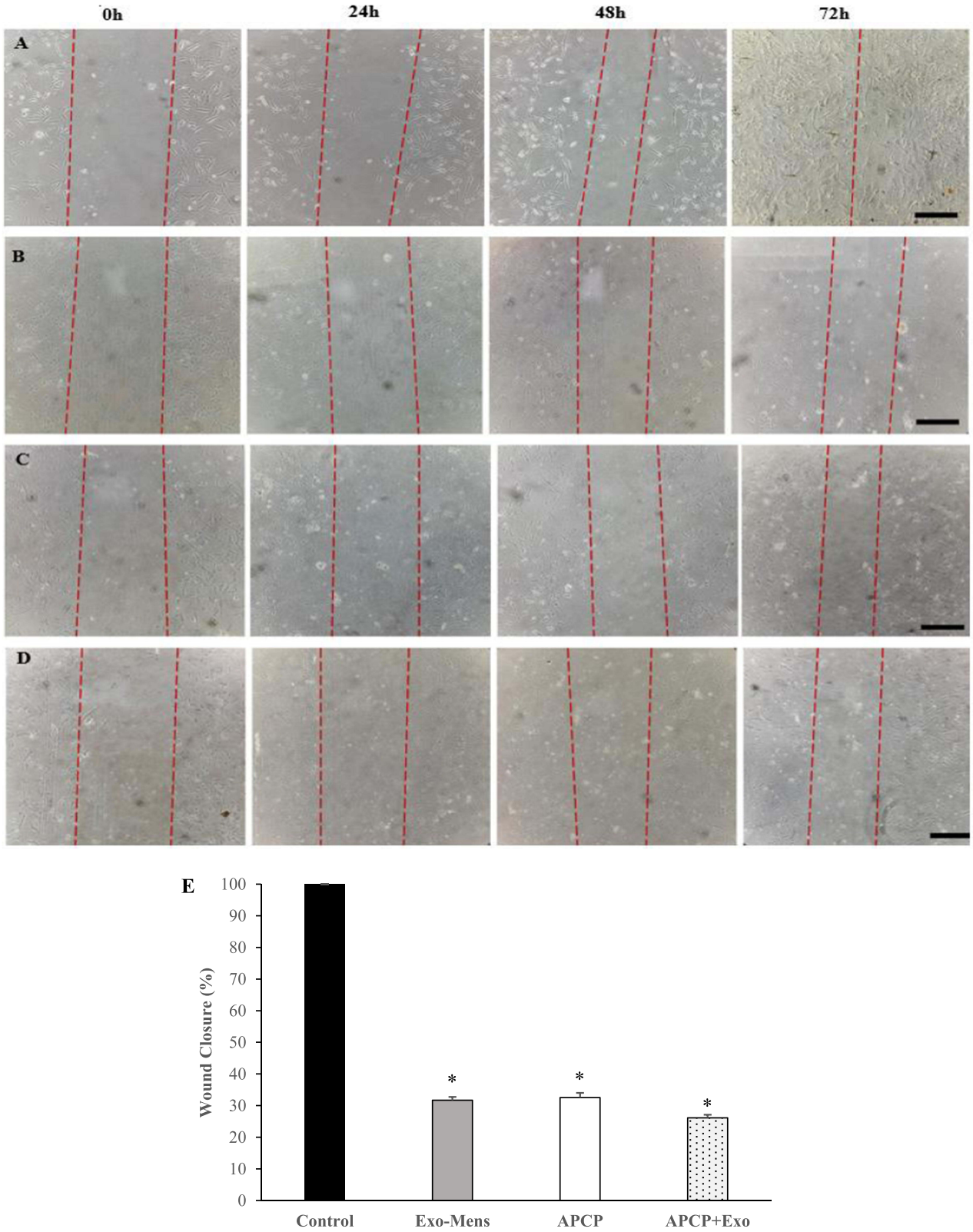

Figure 7 Wound healing assay showing wound closure in SKBR3 cells across treatment groups: control (**A**), Exo-Mens (**B**), APCP (**C**), and APCP+Exo (**D**), monitored at 0, 24, 48, and 72 h. Representative images were obtained at 20× magnification; scale bars denote 200 μm. Red dotted lines delineate the initial wound boundaries at 0 hours in the scratch assay, illustrating progressive cell migration and wound closure over the 72-hour observation period. The percentage of cell migration for each group is quantified in (**E**). Data represent the mean ± SEM of three independent biological replicates performed in triplicate. Statistical analysis: *$p < 0.001$ vs. control group.

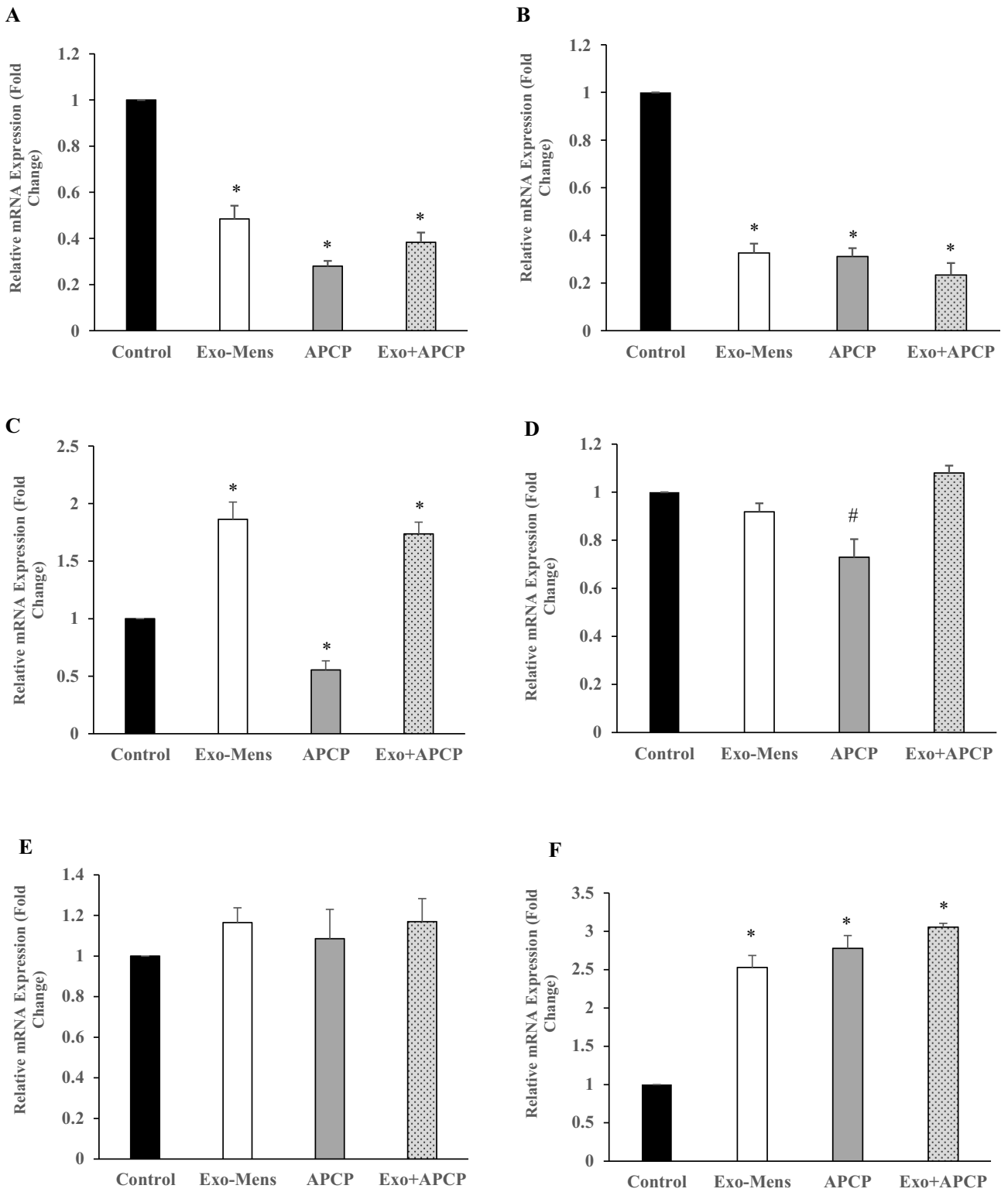

Figure 8 Expression levels of proangiogenic and cancer-related genes—including HIF-1α (**A**), KDR (**B**), NFKB (**C**), MMP9 (**D**), miR-20a (**E**), and miR-422a (**F**)—were measured in response to treatment with Exo-Mens, APCP, APCP+Exo, and in control samples. Results are presented as mean ± SEM from three independent experiments. * $P < 0.001$ and # $P=0.01$ (versus control).

https://doi.org/10.2147/CMAR.S581878

Our investigation into the expression profiles of miR-20a and miR-422a demonstrated that each treatment group increased miR-422a expression in SKBR3 breast cancer cells ($P < 0.001$ for all). Importantly, the increase in miR-422a expression was greater than that of miR-20a. The mean expression levels of miR-20a in the Exo-Mens, APCP, and Exo +APCP groups were 2.52 ± 0.15, 2.77 ± 0.16, and 3.05 ± 0.05, respectively. These results indicate a more robust response of miR-422a to the therapeutic strategies applied, particularly in the combinational treatment group (Figure 8E and F).

Apoptosis Assay

To confirm apoptosis-induced cell death in the examined groups, an Annexin V/Propidium Iodide (PI) assay was performed. The treatment of SKBR3 cells included Exo-Mens, APCP, and Exo+APCP compared with the control group. Flow cytometry analysis revealed that the cell viability in the control group was 89.1%. Conversely, the percentages of non-apoptotic cells (viable cells) in the Exo-Mens, APCP, and Exo+APCP groups were 55.3%, 32%, and 46.2%, respectively (Figure 9). The results highlight the significant effect of the examined groups, particularly APCP, on reducing apoptosis in SKBR3 cells.

Discussion

Despite advancements in targeted therapies, especially in HER2+ BC, the challenges of treatment resistance and tumor recurrence remain significant, highlighting the necessity for innovative and more effective treatment strategies.[30] The tumor microenvironment, especially the adenosinergic signaling pathway facilitated by CD73, is vital for immune evasion, angiogenesis, and the advancement of cancer, positioning CD73 as a potential therapeutic target.[12] On the other hand, exosomes derived from MenSCs have especially gained increasing attention due to their unique bioactive cargo, regenerative potential, and ability to modulate tumor behavior through cell-to-cell communication.[17] This study was therefore designed to explore the synergistic anti-cancer effects of combining a CD73 inhibitor (APCP) with Exo-mens, aiming to overcome limitations of monotherapies, enhance cytotoxicity, and target multiple oncogenic pathways simultaneously. By focusing on the regulation of miR-20a and miR-422a, which are known to play pivotal roles in tumor growth and invasion, our work provides a novel therapeutic approach that addresses both molecular and microenvironmental factors in HER2-positive breast cancer. The present findings provide preliminary evidence supporting the synergistic anti-angiogenic and regulatory effects of combined CD73 inhibition and Exo-Mens treatment in HER2-positive breast cancer cells; however, further in vivo and clinical investigations are required to confirm these mechanisms and therapeutic implications.

The current study findings revealed that the combination of APCP and Exo-Mens not only enhanced cytotoxicity compared to each treatment alone but also may play an important modulatory role in tumor proliferation, migration, angiogenesis, and apoptosis. This synergistic effect was particularly evident in colony formation, wound healing assays, and the regulation of miR-422a, suggesting a multifaceted mechanism of action.

In the TME, various cells, both normal and tumoral, release nucleotides (ATP and AMP) in response to stressors such as injury, hypoxia, and inflammation. Following this, CD39 (ENTPD1) transforms ATP and ADP into AMP, after which CD73 breaks down AMP into adenosine. Beyond its enzymatic role, CD73 also serves as a signaling and adhesion molecule, interacting with extracellular matrix components such as fibronectin and laminin, thereby facilitating cellular migration and invasion.[31] Preclinical evidence demonstrates that CD73 is overexpressed across multiple tumor types, including breast cancer, and its elevated expression correlates with aggressive disease, metastasis, and poor prognosis.[32,33] Significantly, in breast cancer models, especially those driven by HER2, high CD73 expression has been associated with resistance to therapies like trastuzumab, suggesting that CD73 may contribute to therapeutic escape mechanisms.[14] Our results align with previous studies that highlight the ability of CD73 blockade to inhibit tumor growth and sensitize cancer cells to additional treatments. The pronounced reduction in cell viability (IC50 = 12.41 μg/mL for APCP) compared to Exo-Mens (IC50 = 61.84 μg/mL) underscores the potency of CD73 inhibition. However, it has been shown that Exo-Mens can also modulate the tumor microenvironment and offer a unique therapeutic advantage due to their bioactive cargo of proteins, miRNAs, and lipids.[34] In our study, Exo-Mens showed antitumor activity, although less potent than APCP alone. Interestingly, their combination significantly enhanced cytotoxicity, as evidenced by the CompuSyn analysis (combination index < 1 for most Fa values), indicating strong synergy. This is consistent with the

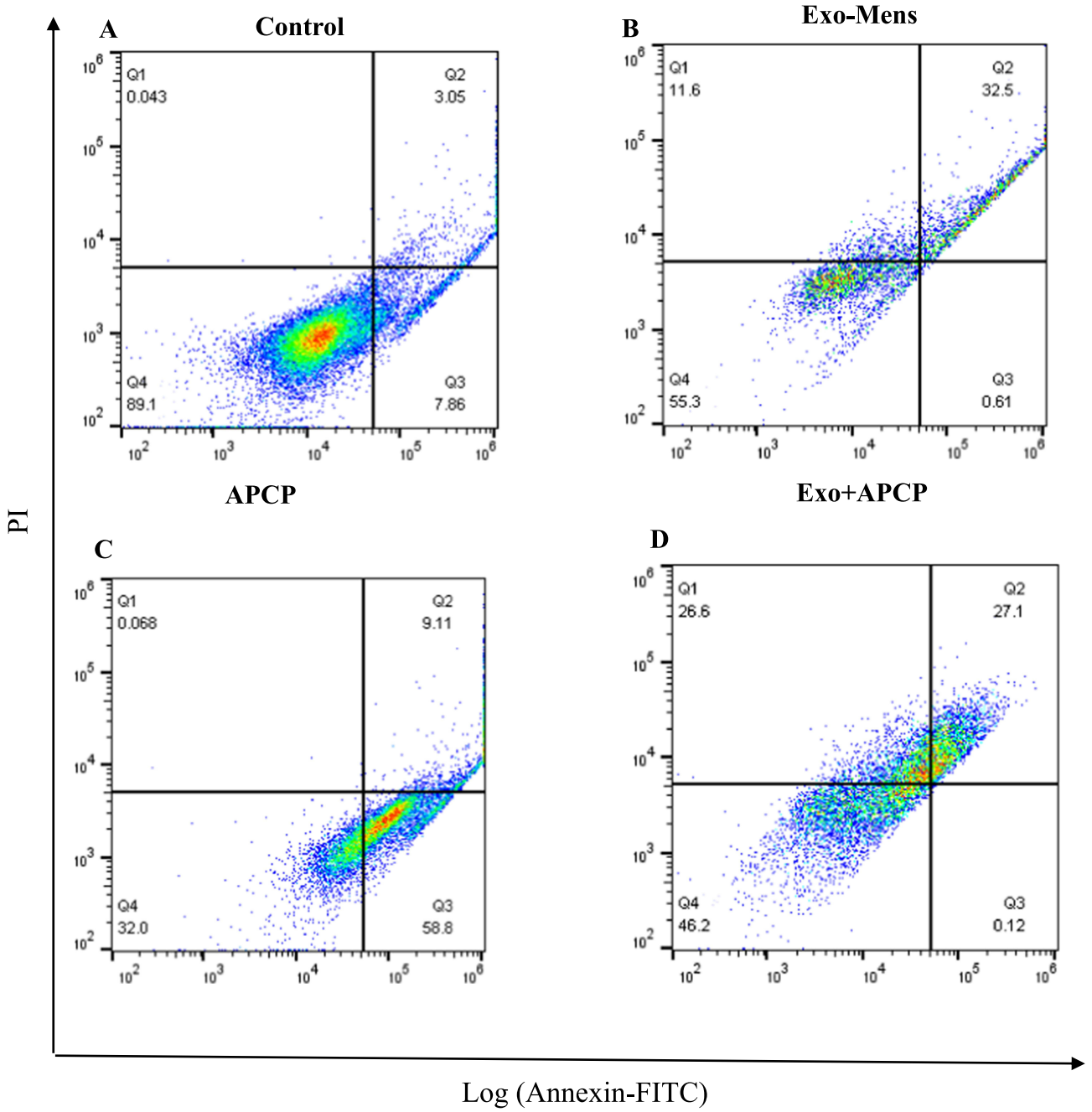

Figure 9 Flow cytometry analysis of SKBR3 cells following 48-hour treatment with Control (**A**), Exo-Mens (**B**), APCP (**C**), and APCP+Exo (**D**). Representative plots demonstrate the distribution of viable cells (Q4: Annexin V–/PI–), early apoptotic cells (Q3: Annexin V+/PI–), late apoptotic cells (Q2: Annexin V+/PI+), and necrotic cells (Q1: Annexin V–/PI+).

concept that exosomes can deliver therapeutic biomolecules while APCP disrupts immunosuppressive adenosine signaling, resulting in a more hostile environment for cancer cell survival.

Consistent with the MTT results, the colony formation assay demonstrated a marked reduction in clonogenic potential with the combined treatment (10.41% colony formation compared to 100% in control), surpassing the effects of individual treatments (36.45% for Exo-Mens and 16.47% for APCP). This may suggest that APCP and Exo-Mens could influence complementary cellular pathways to reduce cell proliferation. Similarly, the scratch assay revealed enhanced inhibition of migration in the combination group, a finding that may have implications, considering the central role of metastatic dissemination in breast cancer progression. The Annexin V/PI assay indicated a trend toward increased

https://doi.org/10.2147/CMAR.S581878

apoptosis, particularly in the APCP-treated group (32% viable cells) compared to Exo-Mens alone (55.3% viable cells). The combination therapy resulted in 46.2% viability, indicating a synergistic apoptotic effect. These findings are consistent with the study by Xiuling Zhi et al, which demonstrated that CD73 suppression in MDA-MB-231 breast cancer cells resulted in G0/G1 cell cycle arrest and induced apoptosis, accompanied by increased TUNEL positivity. Exo-Mens may potentiate this effect by delivering regulatory RNAs and proteins that increase cancer cells' susceptibility to apoptosis. Consistent with the study by Hassannejad et al, exosome treatment significantly increased apoptotic activity and reduced proliferation, migration, and invasion in TNBC (MDA-MB-231) cells, as corroborated by a decrease in colony-forming capacity.[25] In addition, Qian-Yu Liu et al suggested that Exo-Mens suppressed the proliferation and invasion of HeLa cervical cancer cells by inducing G0/G1 cell cycle arrest. They also showed that TGF-β1 released by Mens-MSC inhibits cervical cancer growth in vivo and in vitro by activating JNK/P21 signaling.[35] Studies have been conducted on the role of APCP in cancer, especially breast cancer. Petruk et al, in a study, demonstrated that pharmacological inhibition of CD73 with APCP or genetic silencing via shRNA significantly reduced cell viability, migration, and invasive capacity of TNBC cell lines (MDA-MB-231 and 4T1), even under hypoxic conditions that typically enhance tumor aggressiveness. Jiangang Yu et al also revealed that overexpression of CD73 significantly enhances breast cancer cell proliferation in both in vitro and in vivo models, primarily by activating the AKT/GSK-3β/β-catenin/cyclin D1 signaling cascade.[36] The selection of HER2+ breast cancer models in this study was deliberate, given the established interplay between CD73-mediated adenosine signaling and resistance to anti-HER2 therapies. High CD73 expression has been implicated in promoting immunosuppressive microenvironments that diminish the efficacy of HER2-targeted agents, providing a rationale for exploring CD73 inhibition specifically in this aggressive subtype. Regarding the impact of high CD73 expression in HER2-positive breast cancer, Turcotte et al reported that CD73 plays a key role in reducing trastuzumab response by suppressing immune responses induced by anti-ErbB2 antibodies. Preclinical models also showed that simultaneous targeting of CD73 and HER2 significantly improves therapeutic efficacy and leads to significant inhibition of tumor growth and metastasis.[14]

At the molecular level, our qRT-PCR analysis revealed significant downregulation of angiogenesis-related genes (HIF-1α and KDR) across all treatment groups, with the combination therapy demonstrating the most pronounced effect. This is particularly important since HER2-positive tumors are characterized by high vascularization and aggressive angiogenic signaling. Downregulation of HIF-1α may impair the hypoxia response pathway, while KDR (VEGFR-2) suppression can directly inhibit endothelial cell proliferation and angiogenesis. These results are consistent with previous studies showing that both exosomes and CD73 inhibition can independently affect angiogenic pathways; however, their combination appears to amplify this effect.

Studies have established that the HER2 signaling pathway leads to upregulation of HIF-1α and HIF-2α in breast cancer cells, which in turn enhances the expression of hypoxia-responsive genes such as VEGF and its receptor KDR.[37] These molecules play essential roles in angiogenesis, tumor growth, and treatment resistance. Under hypoxic conditions, HIF activation upregulates CD73 expression, leading to increased extracellular adenosine that promotes an immunosuppressive and pro-angiogenic tumor microenvironment.[38] Inhibiting CD73 with agents like APCP reduces adenosine levels, destabilizes HIF, and downregulates HIF target genes, including KDR, thereby disrupting the positive feedback loop driving angiogenesis. Since KDR plays a critical role in mediating VEGF-driven blood vessel formation, its reduced expression hampers tumor angiogenesis and growth.[13] Our findings of decreased HIF and KDR expression following APCP treatment align with these mechanisms and corroborate existing literature on the interplay between hypoxia, CD73 signaling, and angiogenic regulation in HER2+ breast cancer.[39–42] Interestingly, we observed differential effects on invasion-related genes (MMP9 and NF-κB). While treatment with APCP resulted in a significant decrease in MMP-9 and NF-κB expression, treatment with Exo-Mens increased MMP-9 expression and a slight decrease in NF-κB. However, the combination treatment showed a moderate response. In contrast to our results, Miranda et al showed that exosomes isolated from MenSCs reduced NF-κB activity in prostate cancer.[17] This complex interaction suggests that while exosomes can sometimes enhance pro-invasive signaling, concomitant inhibition of CD73 counteracts this effect, resulting in a net reduction in invasive potential. The subtle interplay between these pathways warrants further mechanistic studies, particularly on the Exo-Mens cargo and its direct effect on NF-κB signaling.

One of the most intriguing findings of our study is the modulation of miR-20a-5p and miR-422a levels. Our findings indicate that although the expression of miR-20a did not show significant changes among the treatment groups, miR-422a was markedly upregulated upon treatment with Exo-Mens, APCP, and the combination of Exo-Mens and APCP (3.05 ± 0.05-fold change). Previous studies indicate that miR-422a functions as a tumor suppressor in multiple cancers, capable of inhibiting cell proliferation, inducing apoptosis, and suppressing metastatic behavior.[20,43] STRING analysis further confirms that miR-422a interacts with important cancer-associated genes, such as SMAD4 and AKT1, both of which are implicated in pathways associated with epithelial-mesenchymal transition (EMT), hypoxia response, and angiogenesis.[44] The significant elevation of miR-422a following treatment may suggest a contribution of this miRNA in modulating tumor cell behavior in HER2-positive breast cancer. However, its precise involvement remains unclear. In contrast, no significant changes in miR-20a expression were observed after treatment. Although previous literature identifies miR-20a as an oncogenic microRNA associated with cancer progression and drug resistance,[45,46] our findings suggest it is not a primary effector in the response to CD73 antibody or Exo-Mens in HER2-positive breast cancer, at least under our experimental conditions. STRING interaction analysis reveals that, although miR-20a targets several cancer-relevant genes (such as MYC and HIF1A), the lack of expression changes limits its therapeutic potential in this context. Collectively, these data indicate that the synergistic application of the CD73 antibody and menstrual blood stem cell-derived exosomes exerts anti-cancer activity predominantly through upregulation of miR-422a and its downstream target genes, rather than through miR-20a. These findings highlight the potential function of miR-422a as a molecular marker and therapeutic agent in the management of HER2-positive breast cancer. Despite these promising findings, several limitations should be noted. This in vitro study was restricted to the SKBR3 HER2+ cell line and may not fully reflect the complexity of the in vivo tumor microenvironment, including immune and stromal interactions. Comparisons with HER2-negative subtypes were not conducted, limiting assessment of effect specificity. Furthermore, the direct causal role of miR-422a upregulation in the observed anti-tumor effects requires additional mechanistic validation. Future studies employing in vivo models, diverse cell lines, and clinical specimens are essential to substantiate these preclinical observations and evaluate translational potential.

Conclusion

This study suggested that combining CD73 inhibition with APCP and exosomal therapy using MenSC-derived exosomes may lead to synergistic effects in this preclinical in vitro model of HER2-positive breast cancer. The combination appeared to reduce tumor cell viability and clonogenic potential, while also potentially consistent with angiogenesis through the downregulation of HIF-1α and KDR, limiting migration, and promoting apoptosis. Notably, the observed upregulation of miR-422a may suggest a tumor-suppressive function, although further studies are necessary to clarify its precise contribution. Taken together, these preliminary in vitro findings provide a rationale for multi-target therapeutic strategies integrating CD73 blockade and exosome-based modulation, offering a basis for further preclinical and clinical validation to assess translational potential in HER2-positive breast cancer.

Abbreviations

BC, Breast Cancer; HER2 / ErbB2, Human Epidermal Growth Factor Receptor 2 / Erythroblastic Oncogene B2 Receptor Tyrosine Kinase 2; NT5E, Ecto-5'-nucleotidase; GPI, Glycosylphosphatidyl Inositol; AMP, Adenosine Monophosphate; ADP, Adenosine Diphosphate; ATP, Adenosine Triphosphate; TME, Tumor Microenvironment; VEGF, Vascular Endothelial Growth Factor; HIF / HIF-1α / HIF-2α, Hypoxia-Inducible Factor / 1 alpha / 2 alpha; MenSCs, Menstrual Blood-Derived Stem Cells; Exo-Mens, Menstrual Blood-Derived Stem Cell Exosomes; ROS, Reactive Oxygen Species; NF-κB, Nuclear Factor kappa-light-chain-enhancer of activated B cells; bFGF, basic Fibroblast Growth Factor; miRNA, microRNA; miR-20a / miR-422a, MicroRNAs 20a and 422a; UTR, Untranslated Region; SMAD4, SMAD Family Member 4; APCP, Adenosine 5′-(α,β-methylene)diphosphate (CD73 inhibitor); PBS, Phosphate-Buffered Saline; cDNA, Complementary DNA; FITC, Fluorescein Isothiocyanate; PI, Propidium Iodide; SEM, Standard Error of the Mean; Fa, Fraction Affected; CI, Combination Index; DRI, Dose-Reduction Index; CompuSyn, Computational Software for Chou–Talalay Method; KEGG, Kyoto Encyclopedia of Genes and Genomes; miRTarBase, microRNA Target Database; MirDB, microRNA Database; PPI, Protein–Protein Interaction; STRING, Search Tool for the Retrieval of Interacting Genes/

Proteins (bioinformatics database); PEG, Polyethylene Glycol; TEM, Transmission Electron Microscopy; DLS, Dynamic Light Scattering; ENTPD1 (CD39), Ectonucleoside Triphosphate Diphosphohydrolase 1; KDR, Kinase Insert Domain Receptor; MMP9, Matrix Metallopeptidase 9; TUNEL, Terminal deoxynucleotidyl transferase dUTP nick end labeling (apoptosis assay); TNBC, Triple-Negative Breast Cancer; AKT, Protein Kinase B (AKT1); GSK-3β, Glycogen Synthase Kinase 3 beta; β-catenin, Beta-catenin signaling protein; Cyclin D1, Cell cycle regulatory protein; EMT, Epithelial–Mesenchymal Transition; MYC, Myelocytomatosis Oncogene; JNK/P21, c-Jun N-terminal Kinase / Cyclin-dependent kinase inhibitor 1 (p21); TGF-β1, Transforming Growth Factor Beta 1.

Ethical Statement

This paper does not contain any studies with human participants or animals.

Acknowledgments

During the preparation of this study, the authors used ChatGPT and Grammarly to improve the clarity and readability of the text and check grammar. After using these tools, the authors thoroughly reviewed, revised, and edited the content to ensure accuracy and appropriateness. The authors take full responsibility for the integrity and originality of the manuscript's content.

Funding

This study was supported by a grant from Motamed Cancer Institute (Grant number: 0220101).

Disclosure

The authors declared no potential conflicts of interest with respect to the research, authorship, and/or publication of this article.

References

1. Mercogliano MF, Bruni S, Mauro FL, Schillaci R. Emerging targeted therapies for HER2-positive breast cancer. *Cancers*. 2023;15(7). doi:10.3390/cancers15071987
2. Marra A, Chandarlapaty S, Modi S. Management of patients with advanced-stage HER2-positive breast cancer: current evidence and future perspectives. *Nat Rev Clin Oncol*. 2024;21(3):185–202. doi:10.1038/s41571-023-00849-9
3. Li J, Li X, Fu R, et al. Recent research advances in HER2-positive breast cancer concerning targeted therapy drugs. *Molecules*. 2025;30(14). doi:10.3390/molecules30143026
4. Pegram M, Jackisch C, Johnston SRD. Estrogen/HER2 receptor crosstalk in breast cancer: combination therapies to improve outcomes for patients with hormone receptor-positive/HER2-positive breast cancer. *Npj Breast Cancer*. 2023;9(1):45. doi:10.1038/s41523-023-00533-2
5. Obidiro O, Battogtokh G, Akala EO. Triple negative breast cancer treatment options and limitations: future outlook. *Pharmaceutics*. 2023;15(7):1796. doi:10.3390/pharmaceutics15071796
6. Yu J, Mu Q, Fung M, Xu X, Zhu L, Ho RJY. Challenges and opportunities in metastatic breast cancer treatments: nano-drug combinations delivered preferentially to metastatic cells may enhance therapeutic response. *Pharmacol Ther*. 2022;236:108108. doi:10.1016/j.pharmthera.2022.108108
7. Antonioli L, Pacher P, Vizi ES, Haskó G. CD39 and CD73 in immunity and inflammation. *Trends Mol Med*. 2013;19(6):355–367. doi:10.1016/j.molmed.2013.03.005
8. Wang L, Zhang J, Zhang W, et al. The inhibitory effect of adenosine on tumor adaptive immunity and intervention strategies. *Acta Pharmaceutica Sinica B*. 2024;14(5):1951–1964. doi:10.1016/j.apsb.2023.12.004
9. Jiang T, Xu X, Qiao M, et al. Comprehensive evaluation of NT5E/CD73 expression and its prognostic significance in distinct types of cancers. *BMC Cancer*. 2018;18(1):267. doi:10.1186/s12885-018-4073-7
10. Angioni R, Liboni C, Herkenne S, et al. CD73 + extracellular vesicles inhibit angiogenesis through adenosine A 2B receptor signalling. *J Extracell Vesicles*. 2020;9(1):1757900. doi:10.1080/20013078.2020.1757900
11. Du X, Ou X, Song T, et al. Adenosine A 2B receptor stimulates angiogenesis by inducing VEGF and eNOS in human microvascular endothelial cells. *Exp Biol Med*. 2015;240(11):1472–1479. doi:10.1177/1535370215584939
12. Shan L, Gong M, Zhai D, Meng X, Liu J, Lv X. Research progress of CD73-adenosine signaling regulating hepatocellular carcinoma through tumor microenvironment. *J Exp Clin Cancer Res*. 2025;44(1):161. doi:10.1186/s13046-025-03416-5
13. Synnestvedt K, Furuta GT, Comerford KM, et al. Ecto-5′-nucleotidase (CD73) regulation by hypoxia-inducible factor-1 mediates permeability changes in intestinal epithelia. *J Clin Invest*. 2002;110(7):993–1002. doi:10.1172/JCI0215337
14. Turcotte M, Allard D, Mittal D, et al. CD73 promotes resistance to HER2/ErbB2 antibody therapy. *Cancer Res*. 2017;77(20):5652–5663. doi:10.1158/0008-5472.Can-17-0707
15. Kang E, Suh S-W, Choi YS, Kim HS, Kim MK. CD39 and CD73 expression in breast cancer: CD73 as a favorable prognostic factor in HER2-positive tumors. *J Breast Cancer*. 2025;28(4):255–267. doi:10.4048/jbc.2025.0040

16. Robalo Cordeiro M, Roque R, Laranjeiro B, Carvalhos C, Figueiredo-Dias M. Menstrual blood stem cells-derived exosomes as promising therapeutic tools in premature ovarian insufficiency induced by gonadotoxic systemic anticancer treatment. *Int J Mol Sci*. 2024;25(15):8468. doi:10.3390/ijms25158468
17. Alcayaga-Miranda F, González PL, Lopez-Verrilli A, et al. Prostate tumor-induced angiogenesis is blocked by exosomes derived from menstrual stem cells through the inhibition of reactive oxygen species. *Oncotarget*. 2016;7(28):44462–44477. doi:10.18632/oncotarget.9852
18. Kordaß T, Osen W, Eichmüller SB. Controlling the immune suppressor: transcription factors and microRNAs regulating CD73/NT5E. *Front Immunol*. 2018;9:813. doi:10.3389/fimmu.2018.00813
19. Fang -L-L, Wang X-H, Sun B-F, et al. Expression, regulation and mechanism of action of the miR-17-92 cluster in tumor cells. *Int J Mol Med*. 2017;40(6):1624–1630. doi:10.3892/ijmm.2017.3164
20. He Z, Li Z, Zhang X, et al. MiR-422a regulates cellular metabolism and malignancy by targeting pyruvate dehydrogenase kinase 2 in gastric cancer. *Cell Death Dis*. 2018;9(5):505. doi:10.1038/s41419-018-0564-3
21. Maldonado E, Morales-Pison S, Urbina F, Jara L, Solari A. Role of the mediator complex and MicroRNAs in breast cancer etiology. *Genes*. 2022;13(2):234. doi:10.3390/genes13020234
22. Théry C, Amigorena S, Raposo G, Clayton A. Isolation and characterization of exosomes from cell culture supernatants and biological fluids. *Curr Protoc Cell Biol*. 2006;30. doi:10.1002/0471143030.cb0322s30
23. Li P, Kaslan M, Lee SH, Yao J, Gao Z. Progress in exosome isolation techniques. *Theranostics*. 2017;7(3):789–804. doi:10.7150/thno.18133
24. Théry C, Witwer KW, Aikawa E, et al. Minimal information for studies of extracellular vesicles 2018 (MISEV2018): a position statement of the international society for extracellular vesicles and update of the MISEV2014 guidelines. *J Extracell Vesicles*. 2018;7(1):1535750. doi:10.1080/20013078.2018.1535750
25. Hasannejad F, Bahraminasab M, Farahmand L, et al. A thermosensitive hydrogel for the sustained delivery of exosomes extracted from menstrual blood mesenchymal stem cells and frizzled antibody on triple-negative breast cancer cells in vitro. *J Drug Delivery Sci Technol*. 2024;101:106144. doi:10.1016/j.jddst.2024.106144
26. Chou T-C, Talalay P. Quantitative analysis of dose-effect relationships: the combined effects of multiple drugs or enzyme inhibitors. *Adv Enzyme Regul*. 1984;22:27–55. doi:10.1016/0065-2571(84)90007-4
27. Liang -C-C, Park AY, Guan J-L. In vitro scratch assay: a convenient and inexpensive method for analysis of cell migration in vitro. *Nat Protoc*. 2007;2(2):329–333. doi:10.1038/nprot.2007.30
28. Hasannejad F, Arab S, Farahmand L, Darvishi B, Bahraminasab M. Design and optimization of thermosensitive injectable alginate-based hydrogels: potential for loading therapeutic compounds. *Iran Polym J*. 2025;34:1285–1303. doi:10.1007/s13726-024-01427-1
29. Chou T-C. The mass-action law based algorithm for cost-effective approach for cancer drug discovery and development. *Am J Cancer Res*. 2011;1(7):925–954. doi:10.1039/C0IB00130a]
30. Swain SM, Shastry M, Hamilton E. Targeting HER2-positive breast cancer: advances and future directions. *Nat Rev Drug Discov*. 2023;22(2):101–126. doi:10.1038/s41573-022-00579-0
31. Xia C, Yin S, To KK, Fu L. CD39/CD73/A2AR pathway and cancer immunotherapy. *Mol Cancer*. 2023;22(1):44. doi:10.1186/s12943-023-01733-x
32. Chen S, Wainwright DA, Wu JD, et al. CD73: an emerging checkpoint for cancer immunotherapy. *Immunotherapy*. 2019;11(11):983–997. doi:10.2217/imt-2018-0200
33. Buisseret L, Pommey S, Allard B, et al. Clinical significance of CD73 in triple-negative breast cancer: multiplex analysis of a Phase III clinical trial. *Ann Oncol*. 2018;29(4):1056–1062. doi:10.1093/annonc/mdx730
34. Kumar MA, Baba SK, Sadida HQ, et al. Extracellular vesicles as tools and targets in therapy for diseases. *Signal Transduct Targeted Therapy*. 2024;9(1):27. doi:10.1038/s41392-024-01735-1
35. Liu Q-Y, Ruan F, Li J-Y, et al. Human menstrual blood-derived stem cells inhibit the proliferation of hela cells via TGF- β 1-mediated JNK/P21 signaling pathways. *Stem Cells Int*. 2019;2019:9280298. doi:10.1155/2019/9280298
36. Yu J, Wang X, Lu Q, et al. Extracellular 5′-nucleotidase (CD73) promotes human breast cancer cells growth through AKT/GSK-3β/β-catenin /cyclinD1 signaling pathway. *Int J Cancer*. 2018;142(5):959–967. doi:10.1002/ijc.31112
37. Jarman EJ, Ward C, Turnbull AK, et al. HER2 regulates HIF-2α and drives an increased hypoxic response in breast cancer. *Breast Cancer Res*. 2019;21(1):10. doi:10.1186/s13058-019-1097-0
38. Li J, Wang L, Chen X, et al. CD39/CD73 upregulation on myeloid-derived suppressor cells via TGF-β-mTOR-HIF-1 signaling in patients with non-small cell lung cancer. *Oncoimmunology*. 2017;6(6):e1320011. doi:10.1080/2162402x.2017.1320011
39. Cao X, Zhu Z, Cao Y, Hu J, Min M. CD73 is a hypoxia-responsive gene and promotes the Warburg effect of human gastric cancer cells dependent on its enzyme activity. *J Cancer*. 2021;12(21):6372–6382. doi:10.7150/jca.62387
40. Saigí M, Mesía-Carbonell O, Barbie DA, Guillamat-Prats R. Unraveling the intricacies of CD73/adenosine signaling: the pulmonary immune and stromal microenvironment in lung cancer. *Cancers*. 2023;15(23):5706. doi:10.3390/cancers15235706
41. Bi C, Patel JS, Liang SH. Development of CD73 inhibitors in tumor immunotherapy and opportunities in imaging and combination therapy. *J Med Chem*. 2025;68(7):6860–6869. doi:10.1021/acs.jmedchem.4c02151
42. Stagg J, Divisekera U, McLaughlin N, et al. Anti-CD73 antibody therapy inhibits breast tumor growth and metastasis. *Proc Natl Acad Sci U S A*. 2010;107(4):1547–1552. doi:10.1073/pnas.0908801107
43. Zou Y, Chen Y, Yao S, et al. MiR-422a weakened breast cancer stem cells properties by targeting PLP2. *Cancer Biol Ther*. 2018;19(5):436–444. doi:10.1080/15384047.2018.1433497
44. Gonzalez DM, Medici D. Signaling mechanisms of the epithelial-mesenchymal transition. *Sci Signal*. 2014;7(344):re8. doi:10.1126/scisignal.2005189
45. Bai X, Han G, Liu Y, Jiang H, He Q. MiRNA-20a-5p promotes the growth of triple-negative breast cancer cells through targeting RUNX3. *Biomed Pharmacother*. 2018;103:1482–1489. doi:10.1016/j.biopha.2018.04.165
46. Liu L, He J, Wei X, et al. MicroRNA-20a-mediated loss of autophagy contributes to breast tumorigenesis by promoting genomic damage and instability. *Oncogene*. 2017;36(42):5874–5884. doi:10.1038/onc.2017.193